JOURNAL OF CATALYSIS 143, 563–572 (1993)

Hydrogenation of Aromatic Hydrocarbons over Supported Pt Catalysts

III. Reaction Models for Metal Surfaces and Acidic Sites on Oxide Supports

SHAWN D. LIN AND M. ALBERT VANNICE

Department of Chemical Engineering, The Pennsylvania State University, University Park, Pennsylvania 16802-4400

Received March 3, 1993; revised May 19, 1993

Sixteen different reaction models were evaluated for benzene and toluene hydrogenation between 317 and 364 K over a family of supported Pt catalysts. For benzene hydrogenation on the Pt surface, only one model was consistent with all the data—that which invoked the addition of the first H atom to the aromatic ring as the rate-determining step (RDS) as well as the concurrent formation of a predominant H-deficient surface species. This model also described toluene hydrogenation on Pt, and the H-deficient species was indicated to be the phenyl (or tolyl) group. To explain the higher rates obtained with acidic supports, a similar model involving spilled-over hydrogen and aromatic molecules adsorbed on acid sites was considered, and it accurately fit the rate data attributed to the support surface. However, another model proposing addition of the second H atom as the RDS on these acid sites and no inhibition by any H-deficient species could not be discounted. The similar activation energies of 12 ± 2 kcal/mol for benzene, toluene, and xylene hydrogenation on Pt and Pd surfaces as well as on acid sites is attributed to the formation of a cyclohexadiene intermediate; for example, 1,3-cyclohexadiene has a positive free energy of formation of 12.4 kcal/mol. This model appears to be general enough to describe the hydrogenation of numerous aromatic molecules over Group VIII metals.

INTRODUCTION

As mentioned in the preceding papers (*1*, *2*), numerous kinetic models have been proposed for benzene hydrogenation over Group VIII metals, and it has tacitly been assumed that the same reaction mechanisms apply to toluene and other aromatic hydrocarbons. A review of the literature reveals that previous models can be placed in four general classifications. The first class invokes a reaction between a hydrogen molecule, either gas-phase or adsorbed, and the reactant aromatic molecule to form either an adsorbed cyclohexadiene or cyclohexene precursor via quasi-equilibrated steps. The rate-determining step (RDS) is assumed to be the transformation of this precursor to either cyclohexadiene or cyclohexene (*3–5*). The second class also involves a reaction between a H_2 molecule and the adsorbed aromatic molecule, but one of the H_2 addition steps to form an adsorbed intermediate, such as cyclohexadiene, is now proposed to be the RDS. The addition of the first H_2 molecule has usually been considered the RDS (*6–11*), but the addition of the third H_2 molecule has also been proposed (*12*). The presence of an inactive aromatic surface species has also been suggested (*8*, *9*). The third class invokes the sequential addition of adsorbed H atoms to the adsorbed aromatic molecule, with the addition of the first (*13*, *14*), the second (*15*, *16*), or the sixth (*13*, *17–19*) H atom having been proposed as the RDS with any preceding additional steps typically assumed to be quasi-equilibrated. The presence of an inactive surface species was again mentioned (*13*). The fourth class also involves the sequential addition of H atoms to the aromatic molecule, but no RDS is assumed (*20–23*);

0021-9517/93 $5.00

however, without additional assumptions quite complicated rate expressions are obtained. A surface dehydrogenation reaction existing concurrently with this sequence has been proposed (*20*). The simultaneous addition of more than one H atom has also been claimed (*24–27*).

The variation of reaction orders with temperature can provide a sensitive and severe test of the validity of proposed reaction mechanisms, yet, surprisingly, such information for Pt has not been previously available. We have studied the reaction kinetics of benzene and toluene hydrogenation between 317 and 364 K over a family of Pt catalysts (*1, 2*), and the capability of these four classes of models to fit our kinetic data was examined in detail (*28*). For hydrogenation only on the Pt surface, a reaction between hydrogen and benzene (or toluene) was chosen as the RDS, then dissociative or nondissociative H_2 adsorption combined with either competitive or noncompetitive H_2 and benzene (or toluene) adsorption, i.e., either one type or two types of surface sites, was assumed. H_2 adsorption as either the RDS or at a rate equal to the surface reaction was also considered. Then the effect of the formation of inactive, H-deficient surface species was also included. The higher specific activities obtained with acidic supports have been attributed to an additional reaction occurring on the oxide surface between adsorbed aromatic molecules and hydrogen spilled over from the Pt surface (*1, 2, 15, 18*), and the aforementioned reaction schemes were examined for their ability to describe these results. In all, 16 different models were examined in depth (*28*). Some could be excluded immediately because of their inability to give the observed reaction orders under any conditions, while others could be rejected after a data-fitting procedure because physically meaningless kinetic parameters were obtained (*28*); none was rejected based only on a residual sum-of-squares comparison. In the following portion of this paper, the reaction sequence on the Pt surface is discussed first and then the reaction on the oxide surface is examined. Only the physically consistent models resulting from this examination are presented here.

DATA FITTING PROCEDURE

To minimize variations due not only to deactivation that occurred during or between partial pressure runs to determine reaction orders but also to the use of different catalyst samples, the raw partial pressure data at a standard set of reaction conditions were compared to the specific activity determined during the Arrhenius run. If a set of data deviated significantly from that expected from the Arrhenius plot, the entire set would be shifted and normalized to this standard activity; however, some uncertainty still remained because deactivation also affected the Arrhenius plots to some extent (see Refs. (*1*) and (*2*)). Regardless, this adjustment provided meaningful partial pressure dependencies at different temperatures and was necessary to achieve consistent data regression. Any deactivation due to a different sample history prior to the partial pressure experiments was minimized in this manner. In all the regression analyses, time units are seconds and pressure units are atmospheres; for example, rate constants are expressed in s^{-1}, i.e., per site, and adsorption constants are expressed as atm^{-1}. Typical data sets have been given in the two preceding papers (*1, 2*).

The fitting of each data set was typically done by nonlinear regression using an SAS computer package on a VM/CMS 370 mainframe computer, which utilized the default Gauss–Newton method and a default criterion of convergence of 10^{-8}, which means that a relative change in the sum of the squared errors smaller than 10^{-8} implies convergence. As the fitting parameters represent physical constants, they were constrained to be positive numbers during the regression iterations. For a model initially containing more than three parameters, assumptions were made to reduce the number of parameters to three. In some models the

rate constants or the adsorption constants were not always extractable as single parameters from the data fitting, thus they remained as a lumped constant and could not be evaluated. Whenever a rate constant or an adsorption constant could be determined, the activation energy or the entropy and enthalpy of adsorption were calculated and compared to thermodynamic guidelines as well as literature data, if available.

DISCUSSION

Hydrogenation on Metal Surfaces

Perhaps the most significant result of this study is the finding that only *one* model could successfully fit the benzene hydrogenation data at all temperatures and also provide physically meaningful parameters. This model assumes dissociative, noncompetitive H_2 adsorption on sites different from those adsorbing benzene (or toluene) with addition of the first H atom as the RDS, and it *necessitates* the inclusion of a concurrent dehydrogenation reaction involving the aromatic reactant molecule to produce H-deficient species on the metal surface. If * represents a hydrogen adsorption site such as a three-fold or four-fold hollow site, and S represents an on-top site on which the aromatic molecule, A, adsorbs, the sequence of elementary steps describing this model is as follows:

$$H_{2(g)} + 2* \overset{K_{H_2}}{\rightleftharpoons} 2H-* \quad (1)$$

$$A_{(g)} + S \overset{K_A}{\rightleftharpoons} A-S \quad (2)$$

$$A-S + H-* \xrightarrow{k} AH-S + *\,(RDS) \quad (3)$$

$$AH-S + H-* \overset{K_1}{\rightleftharpoons} AH_2-S + * \quad (4)$$

$$AH_2-S + 4H-* \overset{K}{\rightleftharpoons} AH_6-S + 4* \quad (5)$$

$$AH_6-S \overset{1/K_{AH_6}}{\rightleftharpoons} AH_{6(g)} + S \quad (6)$$

$$A-S + * \overset{K_{D_1}}{\rightleftharpoons} AH_{-1}-S + H-* \quad (7)$$

$$AH_{-1}-S + * \overset{K_{D_2}}{\rightleftharpoons} AH_{-2}-S + H-* \quad (8)$$

$$\vdots$$

$$AH_{-5}-S + * \overset{K_{D_6}}{\rightleftharpoons} AH_{-6}-S + H-*. \quad (9)$$

Reaction (3) is the RDS, therefore the rate is

$$r = k\theta_{A-S}\theta_{H-*}. \quad (10)$$

The site balance for *-type sites is very straightforward and the surface coverage of H atoms is

$$\theta_{H-*} = \frac{K_{H_2}^{1/2}P_{H_2}^{1/2}}{1 + K_{H_2}^{1/2}P_{H_2}^{1/2}}. \quad (11)$$

If the surface coverages of all partially hydrogenated aromatic species, AH_i-S (those contained in Eqs. (4)–(6)) are assumed to be low, which is valid because of the much higher hydrogenation reactivity of cyclohexadiene and cyclohexene, then the site balance equation for S-type sites involves only the reactant molecule A and the hydrogen-deficient species resulting from the six possible dehydrogenation steps (Eqs. (7)–(9)), and it can be written as

$$1 = \theta_S + \theta_{A-S} + \theta_{AH_{-1}-S} + \theta_{AH_{-2}-S} + \cdots + \theta_{AH_{-6}-S}. \quad (12)$$

Using the series of Eqs. (7)–(9), relationships such as

$$K_{D_1} = \frac{\theta_{H-*}}{\theta_*}\frac{\theta_{AH_{-1}-S}}{\theta_{A-S}} \quad \text{and}$$

$$\theta_{AH_{-1}-S} = \frac{K_{D_1}}{(K_{H_2}P_{H_2})^{1/2}}\theta_{A-S} \quad (13)$$

can be derived and substituted into Eq. (12) to give

$$1 = \theta_S + \theta_{A-S} + \frac{K_{D_1}}{(K_{H_2}P_{H_2})^{1/2}}\theta_{A-S} + \frac{K_{D_1}K_{D_2}}{(K_{H_2}P_{H_2})}\theta_{A-S} + \cdots$$

$$+ \frac{K_{D_1} \cdot \cdot \cdot K_{D_6}}{(K_{H_2}P_{H_2})^3} \theta_{A-S}$$

$$= \theta_S \left[1 + K_A P_A + \sum_{i=1}^{6} \left(\frac{\Pi_{j=1}^{i} K_{Dj}}{(K_{H_2}P_{H_2})^{i/2}} \right) K_A P_A \right]. \quad (14)$$

Thus, the surface coverage of adsorbed benzene (Bz) or toluene (Tol) becomes

$$\theta_{A-S} = K_A P_A \Bigg/ \left[1 + K_A P_A + \sum_{i=1}^{6} \left(\frac{\Pi_{j=1}^{i} K_{Dj}}{(K_{H_2}P_{H_2})^{i/2}} \right) K_A P_A \right], \quad (15)$$

and substituting Eqs. (11) and (15) into rate expression (10) gives

$$r = kK_{H_2}^{1/2}P_{H_2}^{1/2}K_A P_A \Bigg/ \left[(1 + K_{H_2}^{1/2}P_{H_2}^{1/2}) \times \left(1 + K_A P_A + \sum_{i=1}^{6} \left(\frac{\Pi_{j=1}^{i} K_{Dj}}{(K_{H_2}P_{H_2})^{i/2}} \right) K_A P_A \right) \right]. \quad (16)$$

This rate expression contains too many pa-

imposed to simplify the equation, i.e., one of the six possible hydrogen-deficient surface species dominates. The rate equation then reduces to

$$r = kK_{H_2}^{1/2}P_{H_2}^{1/2}K_A P_A \Bigg/ \left[(1 + K_{H_2}^{1/2}P_{H_2}^{1/2}) \times \left(1 + K_A P_A + \left(\frac{K_i^D}{(K_{H_2}P_{H_2})^{i/2}} \right) K_A P_A \right) \right], \quad (17)$$

where K_i^D represents ΠK_{Dj}. If it is further assumed that the hydrogen-deficient species has a much higher surface coverage than Bz (or Tol), that is, if significant inhibition or

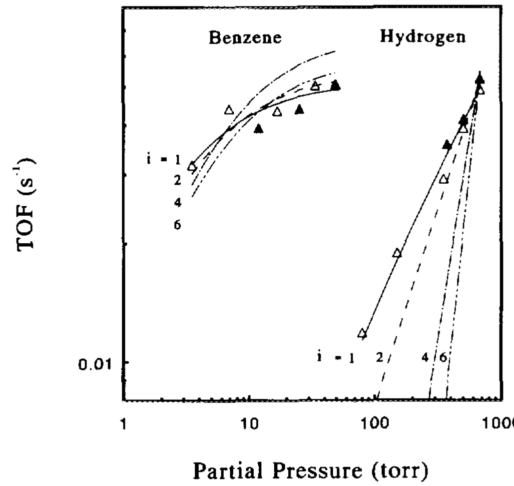

FIG. 1. Benzene hydrogenation over 0.78% Pt/Al_2O_3 at 356 K fitted by Eq. (18) with i = 1, 2, 4, and 6. Symbols represent the data; solid lines represent the fitting with i = 1, while dashed lines represent the fittings with i = 2, 4, and 6. P_{H_2} varied at constant P_{Bz} = 50 Torr, P_{Bz} varied at constant P_{H_2} = 685 Torr.

deactivation is allowed to occur, the final rate equation is obtained:

$$r = \frac{kK_A P_A (K_{H_2}P_{H_2})^{(i+1)/2}}{(1 + (K_{H_2}^{1/2}P_{H_2}^{1/2})[(K_{H_2}P_{H_2})^{i/2} + K_i^D K_A P_A]}. \quad (18)$$

A quick inspection of this equation reveals that the apparent reaction order on the aromatic hydrocarbon can vary between 0 and 1 while the apparent reaction order on H_2 can range between 0 and $(i + 1)/2$, where i represents the number of H atoms lost to form the predominant H-deficient surface species. During the fitting procedure, i was varied from 1 to 6 to determine which species appears to dominate.

Using three fitting parameters—kK_A, K_{H_2}, and $K_i^D K_A$—nonlinear regression of the data at each temperature was conducted, and a set of results at 356 K with i = 1, 2, 4, and 6 is shown in Fig. 1. With i = 1 this model shows a very good fit to the experimental data, while with $i > 1$ this model predicts too strong a dependence on either hydrogen or Bz. Further analysis

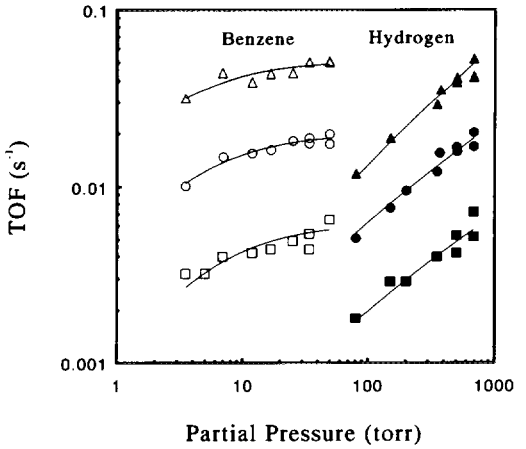

FIG. 2. Benzene hydrogenation over 0.78% Pt/Al_2O_3 at 317 K (△, ▲), 337 K (○, ●), and 356 K (□, ■) fitted by Eq. (18) with $i = 1$. Symbols represent the data. P_{H_2} varied at constant $P_{Bz} = 50$ Torr, P_{Bz} varied at constant $P_{H_2} = 685$ Torr.

showed that this model fits the data well at all three temperatures only when $i = 1$, as shown in Fig. 2, and similar results were obtained with toluene, as shown in Fig. 3. Table 1 lists the sets of regressed parameters for both reactions and the enthalpy and entropy for hydrogen adsorption as determined from the Arrhenius plots of equilibrium adsorption constants shown in Fig. 4.

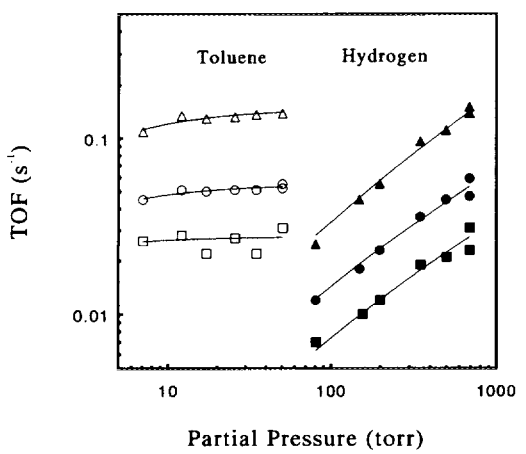

FIG. 3. Toluene hydrogenation over 0.78% Pt/Al_2O_3 at 333 K (△, ▲), 344 K (○, ●), and 364 K (□, ■) fitted by Eq. (18) with $i = 1$. Symbols represent the data. P_{H_2} varied at constant $P_{Tol} = 50$ Torr, P_{Tol} varied at constant $P_{H_2} = 685$ Torr.

The capability of this model to fit the data well at all temperatures demonstrates that it is viable, and additional evidence of its consistency is provided by the thermodynamic values obtained from the fitted equilibrium adsorption constants for H_2. Although there is significant uncertainty, as discussed previously, the apparent heats of adsorption of 10 and 14 kcal/mol H_2 obtained from each reaction are in good agreement with integral values of 13.5 kcal/mol obtained with these Pt catalysts (*29*), and the two entropies of adsorption are also very reasonable (*30*). Furthermore, Tri *et al.* have determined values of 7.2 and 8.9 for relative rates of toluene vs benzene hydrogenation, i.e., relative kK_A values, over Pt/SiO_2 and H_2S-poisoned Pt/SiO_2 catalysts (*31*). From the results in Table 1, we obtain a ratio of 8.7 at an intermediate temperature of 340 K, which again indicates a high degree of consistency with this earlier study.

This proposed model is also consistent with other studies that have appeared in the literature. It was reported years ago that D_2 exchange with aromatic hydrocarbons such as benzene occurred much more rapidly than hydrogenation (deuteration) and proceeded via a different mechanism (*32, 33*). The incorporation of the quasi-equilibrated dehydrogenation steps is consistent with these studies and allows a rapid exchange reaction to occur. In addition, our fitting procedure indicated that the most probable hydrogen-deficient surface species was the phenyl (or tolyl) group. The involvement of phenyl radicals in the exchange reaction has been proposed by Anderson and Kemball (*34*), and recent TPD experiments have shown that both benzene and toluene dehydrogenate on Pt at 400 K and above (*35*). Recent surface science studies have identified phenyl groups formed from benzene adsorbed on Ag(111) (*36*), Os(0001) (*37*), and Ni(111) (*38*) single crystals, and benzyne groups were also proposed to exist on Os (*37*). Thus, the presence of the phenyl group

TABLE 1

Kinetic Parameters and Thermodynamic Properties of Benzene and Toluene Hydrogenation over Pt/Al_2O_3 Obtained from Eq. (18) with $i = 1$

	Benzene				
	Value at:			$-\Delta S^{\circ}_{ad}{}^{a}$ (cal/mol/K)	$-\Delta H^{\circ}_{ad}{}^{a}$ (kcal/mol)
	317 K	337 K	356 K		
kK_A	1.1	5.4	26	—	—
K_{H_2}	85	61	7.4	34 ± 6	14 ± 42
$K_1^D K_A$	1400	1800	920	—	—
	Toluene				
	Value at:			$-\Delta S^{\circ}_{ad}{}^{a}$ (cal/mol/K)	$-\Delta H^{\circ}_{ad}{}^{a}$ (kcal/mol)
	333 K	344 K	364 K		
kK_A	61	41	87	—	—
K_{H_2}	8.8	8.1	2.5	26 ± 2	10 ± 22
$K_1^D K_A$	4600	1500	530	—	—

[a] With 90% confidence intervals.

has precedence even though it has not yet been reported on Pt. Differences in the rate of formation and stability of such H-deficient species, which represent coke precursors, could readily account for the two levels of steady-state activity observed for benzene hydrogenation and the varying degrees of deactivation observed in each reaction (*1*, *2*).

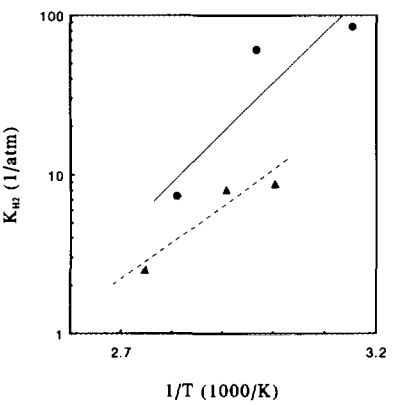

FIG. 4. Variation with temperature of equilibrium adsorption constants obtained from Eq. (18) (from Table 1) for benzene hydrogenation (●) and for toluene hydrogenation (▲) over Pt/Al_2O_3.

The assumption of two different types of adsorption sites on these metal surfaces is not difficult to justify. On surfaces nearly saturated with π-bonded aromatic intermediates, a limited number of sites exist to chemisorb and dissociate H_2, and the H atoms would easily diffuse across these surfaces and would be expected to chemisorb at sites of threefold and fourfold coordination below the aromatic overlayer. Both weakly and strongly bound hydrogen exists on these metal surfaces, and these species can have high surface mobility (*39*, *40*). The π-bonded aromatic species would sit above the metal surface.

Although only this model could fit the benzene data, two other models—those assuming noncompetitive adsorption with no H-deficient species formed, with either the addition of the first H_2 molecule or the second H atom as the RDS—could also fit the toluene results and provide physically meaningful constants with realistic thermodynamic values. Consequently, we cannot reject these models for toluene hydrogenation, but the model presented here in detail for benzene is preferred because it is more

universal, and one of our goals was to provide a unified reaction sequence that is applicable to different aromatic hydrocarbons.

Hydrogenation on Support Surfaces

The higher activity for the hydrogenation of aromatic hydrocarbons when acidic supports are utilized has been established for some time (*15, 20, 41–44*), and the two explanations for this have been either modification of the electronic properties of the metal particles by the support (*41*), or the participation of active sites on the oxide support via hydrogen spillover (*15, 20, 43, 44*). Others have since forwarded similar proposals (*17, 18, 45*). Benzene and toluene adsorption on oxides is well established (*46–52*), and hydrogen spillover is known to occur (*53*); consequently, if adsorption sites for the aromatic molecule are available on the oxide surface and activated hydrogen is present, additional activity can be achieved, particularly in the interfacial region surrounding each metal particle. Thus the total observed rate is the sum of the two contributions—the metal surface and the support.

If one takes the results for the most active (Pt/SiO_2–Al_2O_3) and least active Pt catalysts (Pt/Al_2O_3 and Pt/SiO_2) from the papers preceding this one (*1, 2*) and assumes that the reactions occur only on Pt in the latter two catalysts, then the contribution from the support can be estimated by subtracting the average TOF on Pt/SiO_2 and Pt/Al_2O_3 from the TOF on $Pt/SiO_2 \cdot Al_2O_3$. This gives the rate on the oxide surface normalized to the number of surface Pt atoms present, and if this is done with the partial pressure runs at each temperature, the reaction orders of the rate expression for the $SiO_2 \cdot Al_2O_3$ surface sites can be determined. These results are shown in Figs. 5 and 6. We have verified that the supports alone have no activity under our reaction conditions (*1, 2*), thus the metal component is required to activate the hydrogen, the weakly bound portion of which can migrate readily off the metal onto the oxide surface as an atomic species (*39, 40*).

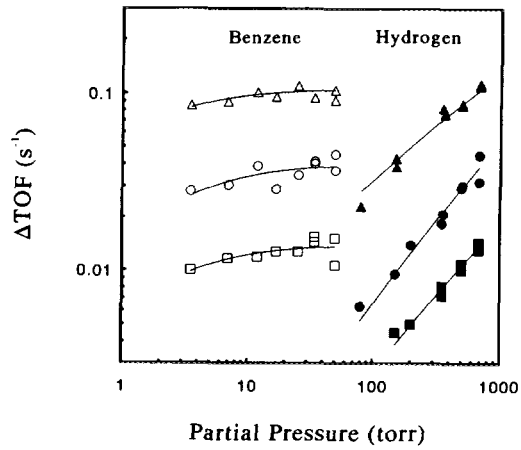

FIG. 5. Hydrogenation activity attributed to the metal-support interfacial region during benzene hydrogenation over 0.24% $Pt/SiO_2 \cdot Al_2O_3$ fitted by Eq. (20) at 317 K (△, ▲), 337 K (○, ●), and 356 K (□, ■). Symbols represent the data.

The two simplest models for hydrogenation on the support involve two limiting possibilities: either H transport from the metal is the slow step or it is very rapid compared to the rate of reaction and is quasi-equilibrated. If the former is assumed, hydrogen

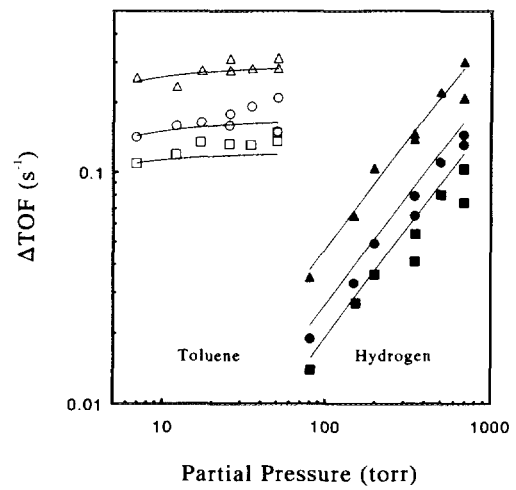

FIG. 6. Hydrogenation activity attributed to the metal–support interfacial region during toluene hydrogenation over 0.24% $Pt/SiO_2 \cdot Al_2O_3$ at 333 K (□, ■), 344 K (○, ●), and 364 K (△, ▲). Curves represent fitting by Eq. (20).

spillover will be proportional to the concentration of H atoms on Pt thus giving an overall reaction order of one-half on H_2. This is inconsistent with the near 1st-order dependence shown in Figs. 5 and 6, so we reject this possibility. If the latter case is assumed, then reaction models identical to those for the Pt surface can be readily obtained—there is just one more equilibrium constant contained in some of the lumped parameters (*28*). On these oxide sites, both benzene and toluene hydrogenation can be described by either of the two models mentioned for toluene hydrogenation on Pt surfaces, i.e., either addition of the second H atom to the reactant aromatic molecule is the RDS and no significant amounts of H-deficient species are assumed, or addition of the first H atom to the reactant molecule is the RDS and a predominant H-deficient species is assumed to coexist on these oxide active sites. The final form of the rate equation for the first model is

$$r = \frac{k' K_S^2 P_{H_2} P_A}{1 + K_A P_A + K_S K_A P_{H_2}^{1/2} P_A}, \quad (19)$$

where k' and K_S are lumped parameters with k' containing the rate constant and K_S incorporating the H spillover term, while K_A represents the equilibrium adsorption constant for the aromatic molecule on the $SiO_2 \cdot Al_2O_3$ surface (*28*). For the second model, the final form is identical to Eq (18) with $i = 1$; it just contains one additional parameter representing the quasi-equilibrated H spillover step, K_S, which multiplies the H_2 adsorption constant, i.e.,

$$r = \frac{k K_A K_S^2 K_{H_2} P_{H_2} P_A}{(1 + K_S K_{H_2}^{1/2} P_{H_2}^{1/2})([K_S K_{H_2}^{1/2} P_{H_2}^{1/2}] + K_I^D K_A P_A)}. \quad (20)$$

We cannot distinguish between them as either fits the data equally well, as shown in Figs. 5 and 6. A value for the equilibrium adsorption constant of the reactant molecule, K_A, on $SiO_2 \cdot Al_2O_3$ at each temperature can be estimated from the first model, and when plotted versus $1/T$ these give quite reasonable values of 17 ± 58 kcal/mol and 36 ± 6 e.u. for the heat and entropy of adsorption for toluene although the uncertainties associated with these values, which represent 90% probability limits, are admittedly high (Q_{ad} values of 15–20 kcal/mol have been reported for toluene on zeolites (*52*). The values of 6 ± 30 kcal/mol and 7 ± 4 e.u. for benzene seem to be too low compared to either the heat of condensation (8.1 kcal/mol) or Q_{ad} values of 12 and 18 kcal/mol reported for benzene adsorbed on H–ZSM5 and NaY zeolites, respectively (*50, 51*). Although the uncertainty limits (again 90% probability limits) of these low values for benzene encompass higher, more reasonable values, these low values could also indicate that the first model is not applicable. Because of the lumped parameters in the second model, no individual Q_{ad} and ΔS_{ad} values could be extracted to further evaluate that model. The numerical values of these fitting parameters are listed elsewhere (*28*).

It is known that H-deficient species are coke precursors and coking can deactivate acid sites in bifunctional catalysts (*54*). Also, Lau and Sermon have reported the formation of carbonaceous deposits on oxides after they were activated by H spillover and used for ethylene hydrogenation (*55*). Consequently, we cannot determine at this time which of these two models is more appropriate; however, the chemistry involved in the hydrogenation sequence is essentially the same. The liquid-phase hydrogenation of aromatic hydrocarbons over noble metals can be catalyzed by the addition of acids via the formation of carbocations (*56–58*); therefore, the proposal in our model that strong acid sites can facilitate hydrogenation has precedent.

One final aspect of this family of reactions is worthy of some discussion—the similarity of the apparent activation energies (ca. 12 ± 2 kcal/mol) regardless of metal, support or aromatic molecule. We attribute this to the necessity of forming cyclohexadiene

(or its analogue, depending on the reactant) during the successive hydrogen addition steps. This compound has a higher free energy due to the destruction of the resonance of the aromatic ring, and by use of a group contribution method a ΔG° value of +12.4 kcal/mol can be calculated for the formation of 1,3-cyclohexadiene from benzene and H_2 (*59*). For comparison, the free energies of formation of cyclohexene and cyclohexane from benzene and H_2 are −5.5 and −23.4 kcal/mol, respectively. It seems apparent that the need to traverse this thermodynamic barrier provides the similarity in activation energies and, for our model to be consistent with this, most if not all, of the energy increase must be associated with the addition of the first H atom to the aromatic ring. This argument favors the addition of the first rather than the second H atom as the RDS, should such a step exist. If reaction orders higher than first order are observed, they can be explained by the formation of different H-deficient surface species. This proposal is quite consistent with earlier work as it is well established that specific activities for hydrogenation of cyclohexadiene or cyclohexene are orders of magnitude greater than that for benzene (*60, 61*).

SUMMARY

A study of benzene and toluene hydrogenation over Pt catalysts at different temperatures has allowed a more complete analysis of reaction models than previously possible because activation energies and heats and entropies could be determined and evaluated. On a Pt surface, only one model was consistent with all the data—that invoking the addition of the first H atom to the aromatic ring as the RDS as well as the presence of a predominant H-deficient surface species, either the phenyl or the tolyl group. The higher specific activities obtained by the use of acidic supports is attributed to the formation of carbocations on acidic sites on the oxide support which react with hydrogen spilled over from the metal surface. This gives an additional contribution to the overall rate, and the same reaction model as that proposed for the metal explains the data if H spillover is assumed rapid compared to the H addition step. This general model accounts for the similarity in apparent activation energies for the hydrogenation of aromatic molecules over noble metals dispersed on both acidic and nonacidic supports, and it provides a unified picture for this family of reactions. Consequently, these models appear to be general enough to be applicable to the hydrogenation of any aromatic hydrocarbon over any of the Group VIII noble metals.

ACKNOWLEDGMENT

This study was supported by the U.S. Department of Energy, Division of Basic Energy Sciences, under Grant DE-FG 02-84ER13276.

REFERENCES

1. Lin, S.-D., and Vannice, M. A., *J. Catal.* **143,** 539 (1993).
2. Lin, S.-D., and Vannice, M. A., *J. Catal.* **143,** 554 (1993).
3. Konyukhov, V. Yu, and Zyskin, A. G., *J. Catal.* **94,** 319 (1985).
4. Murzin, D. Yu., Sokolova, N. A., Kul'kova, N. V., and Temkin, M. I., *Kinet. Katal.* **30,** 1352 (1989).
5. Temkin, M. I., Murzin, D. Yu, and Kul'kova, N. V., *Kinet. Katal.* **30,** 637 (1989).
6. Kehoe, J. P., and Butt, J. B., *J. Appl. Chem. Biotechnol.* **22,** 23 (1972).
7. Merangozis, J. K., Mauntzouranis, B. G., and Sophos, A. N., *Ind. Eng. Chem. Prod. Res. Dev.* **18,** 61 (1979).
8. Völter, J., Hermann, M., and Heise, K., *J. Catal.* **12,** 307 (1968).
9. Fomin, A. A., Granovskii, M. S., Serdyukov, S. I., Safonov, M. S., and Veselkova, O. I., *Kinet. Katal.* **32,** 671 (1990).
10. Klvana, D., Chaouki, J., Kusohorsky, D., Chavarie, C., and Pajonk, G. M., *Appl. Catal.* **42,** 121 (1988).
11. Mirodatos, C., Dalmon, J. A., and Martin, G. A., *J. Catal.* **105,** 405 (1987).
12. Doğu, G., *in* "Proceedings, 8th International Congress on Catalysis, Berlin, 1984," Vol. III, p. 155. Dechema, Frankfurt-am-Main, 1985.
13. Prasad, K. H. V., Prasad, K. B. S., Mallikarjunan, M. M., and Vaidyeswaran, R., *J. Catal.* **84,** 65 (1983).
14. Zrnčević, S., and Rušić, D., *Chem. Eng. Sci.* **43,** 763 (1988).

15. Rahaman, M. V., and Vannice, M. A., *J. Catal.* **127,** 267 (1991).
16. Hartog, F., Tebben, J. H., and Westerings, C. A. M., *in* "Proceedings, 3rd International Congress on Catalysis, Amsterdam, 1964," Vol. 2, p. 1210. Wiley, New York, 1965.
17. Nakano, K., and Kusunoki, K., *Chem. Eng. Commun.* **34,** 99 (1985).
18. Nakano, K., Fueda, Y., Uchino, T., and Kusunoki, K., *J. Chem. Eng. Jpn.* **15,** 397 (1982).
19. Yoon, K. J., and Vannice, M. A., *J. Catal.* **82,** 457 (1983).
20. Chou, P., and Vannice, M. A., *J. Catal.* **107,** 140 (1987).
21. van Meerten, R. Z. C., and Coenen, J. W. E., *J. Catal.* **46,** 13 (1977).
22. Snagovskii, Yu. S., Ljubarskii, G. D., and Ostrovskii, G. M., *Kinet. Katal.* **7,** 258 (1966).
23. Franco, H. A., and Phillips, M. J., *J. Catal.* **63,** 346 (1980).
24. Motard, R. L., Burke, R. F., Canjar, L. N., and Beckman, R. B., *J. Appl. Chem.* **32,** 1 (1957).
25. Canjar, L. N., and Manning, F. S., *J. Appl. Chem.* **12,** 73 (1962).
26. Germain, J. E., Maurel, R., Bourgeois, Y., and Sinn, R., *J. Chim. Phys.* **60,** 1227 (1963).
27. Badilla-Ohlbaum, R., Neuburg, H. J., Graydon, W. F., and Phillips, M. J., *J. Catal.* **47,** 273 (1977).
28. Lin, S.-D., Ph.D. thesis, The Pennsylvania State University, 1992.
29. Sen, B., Chou, P., and Vannice, M. A., *J. Catal.* **101,** 517 (1986).
30. Vannice, M. A., Hyun, S. H., Kalpakci, B., and Liauh, W. C., *J. Catal.* **56,** 358 (1979).
31. Tri, T. M., Massardier, J., Gallezot, P., and Imelik, B., *in* "Studies in Surface Science and Catalysis" (B. Imelik *et al.*, Eds.), Vol. 11, p. 141. Elsevier, Amsterdam, 1982.
32. Hightower, J. W., and Kemball, C., *J. Catal.* **4,** 363 (1965).
33. Harper, R. J., and Kemball, C., *in* "Proceedings, 3rd International Congress on Catalysis, Amsterdam, 1964," Vol. 2, p. 1145. Wiley, New York, 1965.
34. Anderson, J. R., and Kemball, C., *Adv. Catal.* **9,** 51 (1957).
35. Tsai, M.-C., and Meuttereties, E. L., *J. Phys. Chem.* **86,** 5067 (1982).
36. Zhou, X.-L., Castro, M. E., and White, J. M., *Surf. Sci.* **238,** 215 (1990).
37. Graen, H. H., Neumann, M., Wambach, J., and Freund, H.-J., *Chem. Phys. Lett.* **165**(2–3), 137 (1990).
38. Steinrück, H.-P., Huber, W., Pache, T., and Menzel, D., *Surf. Sci.* **218,** 293 (1989).
39. Chen, A. A., Benesi, A. J., and Vannice, M. A., *J. Catal.* **119,** 14 (1989).
40. Sheng, T. C., and Gay, I. D., *J. Catal.* **71,** 119 (1981).
41. Figueras, F., Gomez, R., and Primet, M., *Adv. Chem. Ser.* **121,** 480 (1973).
42. Romero, R. G., and Figueras, F., *C. R. Acad. Sci. Paris C* **275,** 769 (1972).
43. Chou, P., and Vannice, M. A., *J. Catal.* **107,** 129 (1987).
44. Vannice, M. A., and Chou, P., *in* Proceedings, 8th International Congress on Catalysis, Berlin, 1984," Vol. V, p. 99. Dechema, Frankfurt-am-Main, 1985.
45. Coughlan, B., and Keane, M. A., *Catal. Lett.* **5,** 101 (1990).
46. Scurrell, M. S., and Kemball, C., *J. Chem. Soc. Faraday Trans 1* **72,** 818 (1976).
47. McCosh, R., and Kemball, C., *J. Chem. Soc. (A),* 1555 (1968).
48. Lake, I. J. S., and Kemball, C., *Trans. Faraday Soc.* **63,** 2535 (1967).
49. Saunders, P. C., and Hightower, J. W., *J. Phys. Chem.* **74,** 4323 (1970).
50. Pope, C. G., *J. Phys. Chem.* **90,** 835 (1986).
51. Fischer, D. A., Gland, J. L., and Davis, S. M., *Catal. Lett.* **6,** 99 (1990).
52. Tsai, M.-C., and Muetterties, E. L., *J. Am. Chem. Soc.* **104,** 2534 (1982).
53. Conner, W. C., Jr., Pajonk, G. M., and Teichner, S. J., *Adv. Catal.* **34,** 1 (1986).
54. Pieck, C. L., Verderone, R. J., Jablonski, E. L., and Parera, J. M., *Appl. Catal.* **55,** 1 (1989).
55. Lau, M. S. W., and Sermon, P. A., *J. Chem. Soc. Chem. Commun.*, 891 (1978).
56. Skomoroski, R. M., and Schreishiem, A., *J. Phys. Chem.* **65,** 1340 (1961).
57. Wristers, J., *J. Chem. Soc. Chem. Commun.*, 575 (1977).
58. Wristers, J., *J. Am. Chem. Soc.* **97,** 4312 (1975).
59. Danner, R. P., and Daubert, T. E., "Manual for Predicting Chemical Process Design Data." AIChE, New York, 1987.
60. Gonzo, E. E., and Boudart, M., *J. Catal.* **52,** 461 (1978).
61. Smith, H. A., and Meriwether, H. T., *J. Am. Chem. Soc.* **71,** 413 (1949).